

## Coupled channels analysis of $^{12}\text{C}(\pi, \pi)$ at low energy

C. Steven Whisnant\*

*University of South Carolina, Department of Physics and Astronomy, Columbia, South Carolina 29208*

(Received 11 April 1988)

Existing data for the  $0_2^+$  state in  $^{12}\text{C}$  at 50 and 67.5 MeV are compared with coupled channels calculations. Calculations are done with a realistic potential which includes the Lorentz-Lorenz-Ericson-Ericson  $p$ -wave correction and terms second order in the nuclear density. These are compared to results obtained using a phenomenological Kisslinger potential to investigate the sensitivity to the details of the  $\pi A$  interaction. The suppression of the forward angle cross sections by the Lorentz-Lorenz-Ericson-Ericson effect is insufficient to bring the direct transition into agreement at both energies. The interference between the one- and two-step excitation mechanisms is required to reproduce the forward angle data. The dependence of the cross section on the choice of monopole transition density is examined.

### INTRODUCTION

Previous analyses of low-energy pion scattering have shown that monopole transitions are sensitive to both the distorting potential and the treatment of the reaction dynamics.<sup>1-5</sup> These investigations have focused primarily on the 7.65 MeV  $0_2^+$  state in  $^{12}\text{C}$  for which there is extensive nuclear structure information from electron scattering.<sup>6-9</sup> Both distorted wave (DW) and coupled channels (CC) calculations have successfully described the existing  $\pi^+$  data for this state at 50 (Refs. 1 and 3) and 67.5 (Ref. 10) MeV. The CC analyses have demonstrated that the cross sections are dramatically lowered, particularly at angles less than  $60^\circ$ , by the interference of one- and two-step excitation mechanisms. The more recent DW results, however, indicate that this is not necessary. By including the Lorentz-Lorenz-Ericson-Ericson (LLEE) correction to the  $p$ -wave part of the interaction, the required suppression of the cross section is achieved.

This ambiguity exists for several reasons. Different analyses of the  $^{12}\text{C}$  data have used different shapes for the monopole transition density. Although the  $0_2^+$  form factor is known up to a momentum transfer of more than  $3 \text{ fm}^{-1}$ , frequently only the matrix element and the transition radius are used to fix the parameters. Even using all the data to determine the parameters, considerable modifications of the transition densities are permitted. While these variations may be of interest in themselves, they obscure the dependence on the interaction.

These uncertainties are magnified by the restricted nature of earlier investigations. The CC analysis of Sparrow and Gerace<sup>1</sup> focused on the differences between the CC and DW results but made little effort to reproduce the elastic scattering data. The DW analysis of Lee *et al.*<sup>3</sup> fit the optical-model parameters to the  $\pi^+$   $^{12}\text{C}$  data at the one energy of interest, and focused on the effects of including the LLEE correction. To assess the consequences of omitting this correction entirely, the authors compared it to a Kisslinger potential similarly determined by a fit to one data set. The parameters in these

zero-range potentials are strongly correlated,<sup>11-13</sup> making it difficult to evaluate this comparison. While such analyses are a logical first step in examining monopole transitions, important systematics cannot be addressed.

To extend these investigations, data from both 50 and 65 MeV are included here in a systematic analysis. The energy dependence of the angular distribution provides an important constraint on the calculation. Over this relatively small span of energy, the  $\pi A$  interaction changes very little. If direct excitation alone is responsible for the  $0_2^+$  cross section, one would expect the energy variations to be dominated by the changes in the momentum transfer sampled. However, if one- and two-step interference is important a more complicated behavior is anticipated, since the interfering parts have different momentum transfer dependences. Comparing the full calculation with only the direct excitation from the same CC calculation allows an unambiguous comparison of the two methods.

In the absence of a viable field theory for pion-nucleus interactions, phenomenological optical models are used. Because of the success describing resonance energy scattering and pionic atom data, low-energy calculations are done with zero-range potentials. Systematic studies of elastic scattering have demonstrated that zero-range potentials can be found which account for both  $\pi^+$  and  $\pi^-$  elastic data below 100 MeV for a wide range of target masses.<sup>11-16</sup> These potentials have also been shown to give reasonable descriptions of scattering to the  $2_1^+$  states in  $^{12}\text{C}$ ,<sup>28,30</sup>  $^{32}\text{Si}$ , and  $^{32,34}\text{S}$ .<sup>17-19</sup> In these instances the assumption of a zero-range potential appears to be well justified. It is not clear to what extent this assumption is valid in the nuclear interior. One way to examine this question is through the study of monopole transitions. As discussed in the following, monopole transition densities are peaked in the nuclear interior, accentuating density-dependent effects.

The CC calculations are done with two choices of optical model: a realistic potential which accounts explicitly for true pion absorption, the LLEE effect and Pauli blocking, and a purely phenomenological modified Kiss-

linger potential with energy-dependent parameters. It has been demonstrated that for certain regions of parameter space these two potentials give similar results for elastic scattering.<sup>11-13,16</sup> Thus, the comparison is made between two potentials which give approximately equivalent total  $s$ - and  $p$ -wave strengths and reproduce elastic scattering data for more than one energy (and more than one target) with both pion charges.

Finally, calculations are done with monopole transition densities which describe the electron scattering data with momentum transfers up to  $\approx 2 \text{ fm}^{-1}$ . This greatly reduces the ambiguity in this density, giving more confidence that it is the interaction being examined. To

$$-4\pi \left[ p_1 b_0 \rho(r) + p_2 B_0 \rho^2(r) + \frac{1}{2}(1-p_1^{-1}) \nabla^2 c_0 \rho(r) + \frac{1}{2}(1-p_2^{-1}) \nabla^2 C_0 \rho^2(r) - \nabla \frac{L(r) \nabla}{1+4\pi\lambda L(r)/3} \right],$$

where  $p_1$  and  $p_2$  are kinematic factors,  $\rho(r)$  is the nuclear density [ $4\pi \int \rho(r) r^2 dr = A$ ], and  $L(r)$  and  $\lambda$  describe the LLEE effect.

The parameter set "E" (Ref. 15) describes  $\pi^+$  data quite well, but  $\pi^-$  data are not as well reproduced. This deficiency is attributed to the absence of  $\pi^-$  scattering data as a constraint in determining the parameters.<sup>20,21</sup> To remedy this,  $b_0$ ,  $c_0$ , and  $\lambda$  have been adjusted to fit  $\pi^\pm$  elastic scattering from  $^{28}\text{Si}$  and  $^{12}\text{C}$  at 50 MeV.<sup>19</sup> This modified version of the MSU potential, referred to here as MSUT, not only fits the elastic scattering data, but also reproduces the  $^{12}\text{C}$  total reaction cross sections at 50 MeV.

The extension of this model to energies other than those specified by the original authors is usually done by either linear interpolation for energies below 50 MeV or by only changing the first-order parameters which are taken from  $\pi$ -nucleon phase shifts. In the present case, neither method applies. Extrapolation by varying one subset of the parameters is as good as varying another, and all choices are somewhat arbitrary. Having made the decision to modify the first-order parameters to fit the 50 MeV data, the model cannot be extended to 65 MeV by simply scaling with the impulse approximation. In the absence of a detailed theoretical examination and an extensive program of parameter adjustment, the same parameters are used at both energies. While this does not give as good agreement with the data at the higher energy, as will be seen in the following, the modest energy range spanned and the uncertainties in the elastic data at the higher energy do not warrant a detailed fitting of parameters.

For comparison, calculations are also done with a modified Kisslinger potential (MKIS) of the form

$$-K^2 b_0 \rho(r) + b_1 \nabla \rho(r) \nabla - \frac{1}{2} \epsilon b_1 \nabla^2 \rho(r),$$

where  $K$  is the center-of-mass pion wave number and  $\epsilon$  is the total pion center-of-mass energy divided by the nucleon mass. This form for the potential is similar to first-order potentials used in previous investigations of monopole scattering. Here, however, the parameters are

indicate the sensitivity which monopole transitions have to the choice of density and the uncertainty this introduces, calculations are presented with two choices of density.

## OPTICAL MODELS

A theoretically well-motivated, global analysis of elastic scattering has been done by Stricker, McManus, and Carr.<sup>11,14,15</sup> This potential, the so-called Michigan State University (MSU) potential, has been widely used to examine both elastic and inelastic scattering. In the notation of Ref. 15, for  $T=0$  nuclei it has the form

chosen purely phenomenologically by fitting energy-dependent parameters to data over a range of energies and targets. This procedure is described in detail in Ref. 16. Without constraints on the fit to limit the size of the  $p$ -wave strength, it becomes too large. The upper limit is determined by the location of the well-known Kisslinger singularity.<sup>22,23</sup> In the MSUT potential, this reduction of the  $p$ -wave strength is accomplished by including the LLEE effect. Without the density-dependent reduction produced by this correction, a static limit must be imposed to ensure meaningful results. With this limit, the requirement of unitarity and reasonable conditions on the algebraic sign of the imaginary  $s$ -wave strength, fits have been made to  $\pi^\pm$  elastic scattering from even-even nuclei from  $^{12}\text{C}$  to  $^{40}\text{Ca}$  spanning the low-energy region.<sup>16,5</sup> This choice of parameters has been shown to produce a potential which is "equivalent" to the MSU potential for a wide range of energies and can provide a consistent analysis of inelastic scattering from  $^{12}\text{C}$  in a CC framework.<sup>5,16,18</sup>

Comparing the MKIS and MSUT potentials ensures that a meaningful comparison is made between two smoothly varying, nonsingular potentials. Only in this way can the differences in the radial dependence introduced by the higher-order corrections be clearly examined.

The modified harmonic oscillator shape is used for both optical models but with different choices of parameters. The density parameters used in the MSUT potential are taken from the original paper describing this model.<sup>11</sup> These parameters are adjusted away from the electron scattering values to correct for the finite size of the proton. The density parameters used in the MKIS calculations do not include this correction and use parameters taken directly from electron scattering.<sup>24</sup> The potential and density parameters used in the calculations presented here are given in Table I.

The CC calculations were done with a modified version of the code CHOPIN. This code only includes contributions to the transition potential which are first order in the deformation. To this order there is no difference between the excitation of a quadrupole phonon in the vibra-

TABLE I. The parameters used in the MSUT and MKIS potentials for the calculations presented here.

MSUT		MKIS	
$b_0$ (fm)	$-0.064+i0.0029$	50 MeV: $b_0$ (fm <sup>3</sup> )	$-1.931+i0.04644$
$c_0$ (fm <sup>3</sup> )	$0.621+i0.105$	$b_1$ (fm <sup>3</sup> )	$5.619+i1.428$
$B_0$ (fm <sup>3</sup> )	$-0.02+i0.11$	65 MeV: $b_0$ (fm <sup>3</sup> )	$-1.439+i0.04644$
$C_0$ (fm <sup>6</sup> )	$0.36+i0.54$	$b_1$ (fm <sup>3</sup> )	$5.715+i1.598$
$\lambda$	1.41		
$\rho(r)=\rho_0[1+\alpha(r/c)^2]e^{-(r/c)^2}$			
$\alpha$	1.33		1.247
$c$ (fm)	1.57		1.649

tional model and the excitation of the  $2^+$  member of the ground-state rotational band. Since the higher-order terms which differentiate these models are absent, the calculations presented here implicitly assume the vibrational model. The transition potential is given by

$$V^{\text{tr}} = \delta\rho \frac{dV^{\text{el}}}{d\rho},$$

where  $V^{\text{el}}$  is the MSUT or MKIS potential and  $\delta\rho$  is the transition density. For the  $2_1^+$  state this density is given by the derivative of the ground-state density as in the DW analysis.<sup>3</sup> The choices for the monopole transition and the coupling between excited states are discussed in the following.

#### THE GROUND AND $2^+$ STATES

The calculated elastic cross sections are shown in Figs. 1 and 2. At both 50 and 65 MeV the MKIS calculations

are lower than the MSUT for angles larger than  $\approx 60^\circ$ . These smaller values agree with the 65 MeV data of Blecher *et al.*<sup>26</sup> but underestimate the 50 MeV data. One reason for the better agreement at 65 MeV is that this data set was included in the fit and the 50 MeV data were not. No data for  $^{12}\text{C}$  at 50 MeV were used to determine the MKIS parameters because of the enhanced sensitivity seen at this energy to coupling to the  $2_1^+$ . This sensitivity, important for angles less than  $60^\circ$ , arises in  $\pi^+$  from the interference of the Coulomb and hadronic amplitudes.<sup>18</sup> In a DW calculation both potentials underestimate the 50 MeV data in this angular range. These CC calculations, which include coupling to the  $2^+$  (and the  $0_2^+$  as discussed in the following section), effectively increase the imaginary  $s$ -wave strength, giving agreement with the data.

Fitting the smoothly varying MKIS parameters to the elastic data at energies above and below 50 MeV results in a  $p$ -wave strength that is somewhat small at this ener-

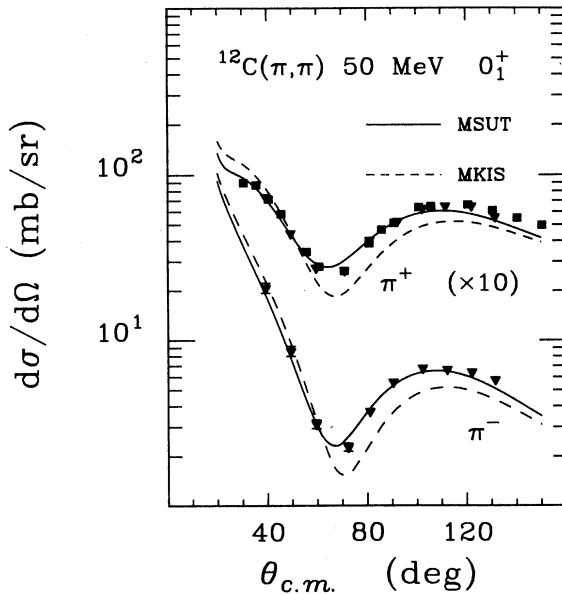


FIG. 1. Elastic scattering from  $^{12}\text{C}$  at 50 MeV. The data are from Refs. 24 (triangles) and 25 (squares). The solid line represents the MSUT results and the dashed line shows the MKIS calculations.

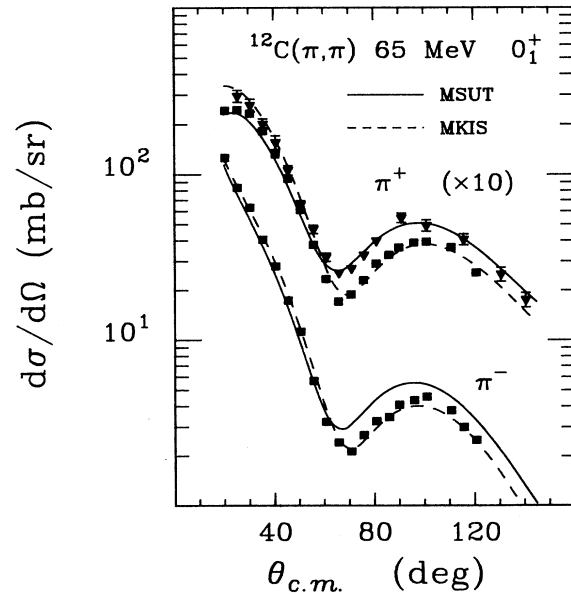


FIG. 2. Elastic scattering from  $^{12}\text{C}$  at 65 MeV. The data are from Ref. 26 (squares) and 10 (triangles). The calculations are labeled as in Fig. 1.

gy. This same behavior was seen in previous analyses with this potential.<sup>16,18</sup> Certainly, this discrepancy may be compensated by relaxing the constraint on the maximum  $p$ -wave size and readjusting the parameters. This will, however, produce a singular, unphysical potential. The calculations presented here indicate the limitations of a systematically determined, nonsingular Kisslinger potential.

As noted in the preceding section, a unique extension of the MSUT potential to 65 MeV is not possible. The discrepancy between the 65 and 67.5 (Ref. 10) MeV data is much larger than a few MeV variation in the calculations can accommodate. This theoretical and experimental uncertainty precludes a detailed fit to the data at this energy. Thus, the same parameters are used for the MSUT potential at both 50 and 65 MeV.

Figures 3 and 4 show the results for the  $2_1^+$  state at 4.439 MeV. The deformation length,  $\beta_2 R$ , is 1.24 fm. This is taken from the previous CC analysis of 50 and 100 MeV data.<sup>18</sup> The same  $\beta_2 R$  is used for both calculations. There is no clear consensus in the literature for the value of this parameter. The values obtained from alpha,<sup>28</sup> proton,<sup>29,30</sup> and electron<sup>28,29</sup> scattering show a wide variation with probe and energy. These range from 1.146 to 1.388 fm obtained from an analysis of alpha scattering at energies between 104 and 1370 MeV, to 1.53–1.68 fm from electron and 40 MeV proton scattering, and to 1.91 fm as determined both from 800 MeV proton scattering and electron scattering. The deformation length used here gives consistent results for pion scattering in the energy range of interest.

The MSUT calculations give excellent agreement with

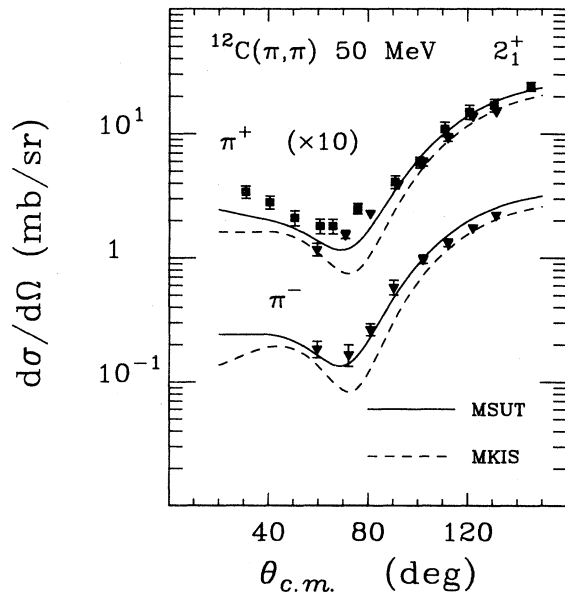


FIG. 3. Scattering to the  $2_1^+$  state at 50 MeV. The data are from Refs. 24 (triangles) and 27 (squares). The calculations are labeled as in Fig. 1.

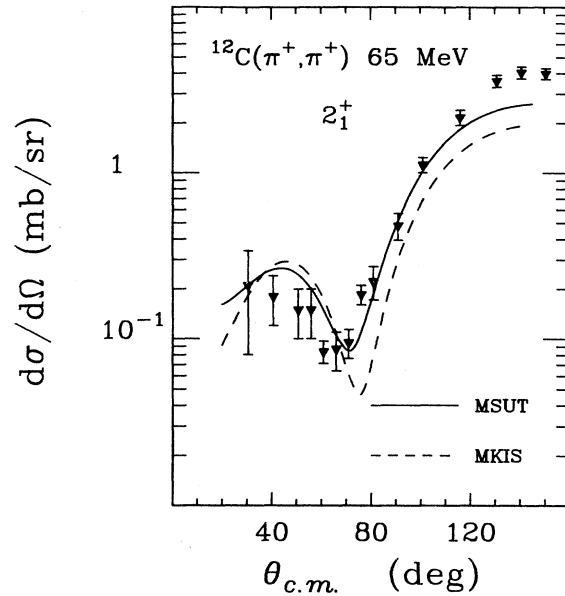


FIG. 4.  $\pi^+$  scattering to the  $2_1^+$  state at 65 MeV. The data are from Ref. 10. The calculations are labeled as in Fig. 1.

the data, even for angles less than the  $s$ - and  $p$ -wave interference minimum. DW analyses with similar potentials typically produce angular distributions which have a ratio of backward angle to forward angle cross sections that is too small.<sup>4,17</sup> Including the coupling back to the ground state removes sufficient strength at forward angles to bring the calculations into accord with the data.

The MKIS cross sections are systematically lower than the data. The earlier CC calculations for  $^{12}\text{C}$  with this potential gave much better agreement than is seen here. As already noted, the present calculations include coupling between the  $2_1^+$  and the  $0_2^+$  states, as well as between these states and the ground state. This removes strength from the  $2_1^+$ , bringing the MSUT cross section down into agreement with the data and lowering the MKIS result below the data. Agreement with the data can be improved by choosing the  $\beta_2 R$  values for the two calculations to be different. However, the monopole transition is very sensitive to both the optical model and the nuclear structure model. Choosing the same deformation length for both calculations reduces the ambiguity in the comparison with the  $0_2^+$  data. A consistent treatment of the couplings means the differences between the resulting monopole cross sections are more clearly due to the choice of potential.

#### THE MONOPOLE TRANSITION

In the full CC calculation, the  $0_2^+$  is coupled to both the ground state and to the  $2_1^+$  state. The nature of these transitions depends on the nuclear structure model adopted. As has been done in previous DW and CC calculations for pion scattering to this state, a vibrational model is assumed. A collective model of low-energy

monopole transitions can be made by choosing a form which respects the orthogonality of the initial and final states and reproduces the known electromagnetic data.<sup>31</sup> In a first-order vibrational model, as assumed here, this is equivalent to treating the  $0_2^+$  state as a one-phonon (breathing mode) oscillation. Ingemarsson and Jonsson have shown that the form factor found from electron scattering is well described by such a one-phonon model. This analysis does not, however, exclude a large admixture of the two-phonon component.

In a simple harmonic vibrator model the  $0_2^+$  state is a two-phonon state and is excited by the successive creation of two quadrupole phonons. Creation of the first phonon produces the  $2_1^+$  state, and the creation of the second gives rise to the characteristic  $0_2^+, 2_2^+, 4_1^+$  triplet at approximately twice the energy of the  $2_1^+$  state. In this approximation the coupling of any of the two-phonon states to the one-phonon state is the same as the coupling between the ground (zero-phonon) and one-phonon states. The radial shape of the transition density is independent of the spin of the initial and final states; it depends only on the angular momentum transfer. This is the model assumed in previous CC analyses for the transition between excited states.

These two ways of describing the  $0_2^+$  state are combined by noting that analyses of alpha<sup>28</sup> and antiproton<sup>32</sup> scattering both indicate that this is a mixed one- and two-phonon state. In the calculations presented here, the coupling to the ground state is effectively through both components of the wave function, being a fit to electron scattering data, but the  $2_1^+ \rightarrow 0_2^+$  coupling is only through the two-phonon component.

In the analysis of antiproton scattering, this model of the transition between excited states was compared with a transition density derived from shell model wave functions. The shell model transition density has a node near the surface. In the language of the vibrational model this indicates that the excited states couple through both the one- and two-phonon components of the  $0_2^+$  wave function. At momentum transfers larger than  $\approx 1 \text{ fm}^{-1}$  the antiproton data are better described using the shell model transition density. However, for smaller momentum transfers the calculated cross sections are similar. Given the small momentum transfer range sampled by the pion data and the large uncertainties in the higher energy data, this refinement in the model is omitted here. The coupling between excited states is assumed to have the same strength and radial dependence as between the  $2^+$  and ground states.

There are many possible choices for the monopole transition density. Two have been selected for the present investigation. The first, from the analysis of Ingemarsson and Jonsson,<sup>28</sup> is derived from a two-parameter Fermi density. The second, also fit to electron scattering data, was used in a previous analysis of pion scattering by Sparrow and Gerace,<sup>1</sup> is derived from a modified harmonic oscillator shape. Calculations using these densities give an indication of the uncertainties introduced by incomplete knowledge of the form factor. Since the two densities are most significantly different in the nuclear interior, this comparison also provides an in-

dication of the sensitivity these transitions have to the nuclear interior.

The model of Ingemarsson and Jonsson (IJ) for the monopole transition density is based on a two-parameter Fermi shape for the nucleus. By allowing the radius  $R$ , the diffuseness  $a$ , and the normalization to be independent parameters, a form was obtained which best fit the electromagnetic data. This density is given by

$$\delta\rho_0(r) = -\frac{\delta R}{R} \left\{ [R + cx(r-R)] \frac{\partial\rho(r)}{\partial r} - (1+x)f\rho(r) \right\},$$

where

$$c = \frac{3R^2 + (\pi a)^2}{2R(\pi a)^2},$$

$$f = \frac{3R^2 + (\pi a)^2}{R(R^2 + (\pi a)^2)},$$

and  $x$  is chosen so that

$$\left. \frac{\partial\delta\rho_0(r)}{\partial r} \right|_{r=0} = 0.$$

The parameters obtained by Ingemarsson and Jonsson which best fit the form factor are  $R = 2.24 \text{ fm}$ ,  $a = 0.47 \text{ fm}$ , and a deformation length,  $\delta R = 0.35 \text{ fm}$ . The present calculations use a normalization which differs by a factor of  $\sqrt{4\pi}$  from their analysis. The calculations presented here were done with  $\delta R = 0.1 \text{ fm}$ .

Figures 5 and 6 show the full CC calculation compared with the  $\pi^+$  monopole data. At 50 MeV the two-step

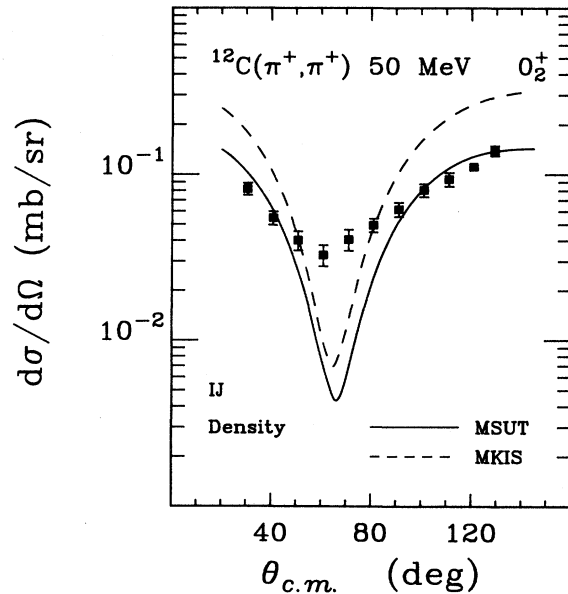


FIG. 5.  $\pi^+$  scattering to the  $0_2^+$  state at 50 MeV. The monopole transition density is given by the Ingemarsson and Jonsson (IJ) model. The curves indicate the MSUT (solid) and MKIS (dashed) calculations when all possible couplings among the  $0_1^+$ ,  $2_1^+$ , and  $0_2^+$  states are included.

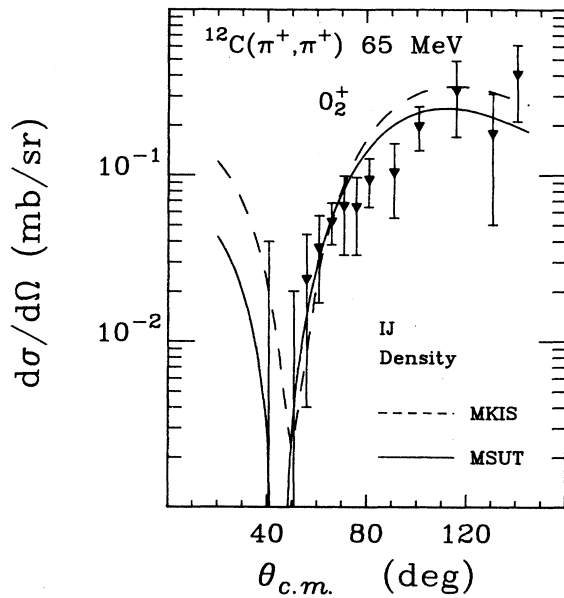


FIG. 6. Same as Fig. 5 for 65 MeV. The data are from Ref. 10.

contribution produces a deeper minimum than is seen in the data. This is also true in the calculation of the monopole cross section in  $^{28}\text{Si}$  at this energy.<sup>5</sup> At forward and backward angles, however, the MSUT calculation reproduces the magnitude of the data quite well. The MKIS potential gives a cross section as much as a factor of 2 larger than the data at these angles. The DW analysis of these data has shown that the LLEE effect is responsible for the suppression at forward angles.<sup>3</sup> The couplings between excited states do not eliminate this suppression. The less dramatic difference between the two calculations in the present analysis than was seen before results from the choice of a weaker Kisslinger potential.

At 65 MeV both calculations give excellent agreement with the data. Where the results differ most, at angles less than  $45^\circ$ , there are no data. The shallow minimum in the data at  $\approx 65^\circ$  at 50 MeV has shifted to  $\approx 45^\circ$  and deepened considerably. This trend is well reproduced by both potentials.

To examine in detail the effect of the one- and two-step interference on this transition, the cross sections produced by the separate contributions are shown in Figs. 7 and 8. The direct excitation with the MSUT potential overestimates the data at forward angles, in contrast to that previously found for a potential including the LLEE correction.<sup>3</sup> This earlier investigation, however, chose the LLEE parameter  $\lambda$  by fitting it to the  $\pi^+$  elastic data at 50 MeV. The  $p$ -wave contained no second-order terms as included here, and a larger  $\lambda$  was required to reduce the large first-order strength. Their value of  $\lambda=1.5$  is 6.4% larger than the value used here. This and the different first-order strength give a real  $p$ -wave strength 15–20% smaller than that used here. At the forward angles where the direct transition is dominated by distur-

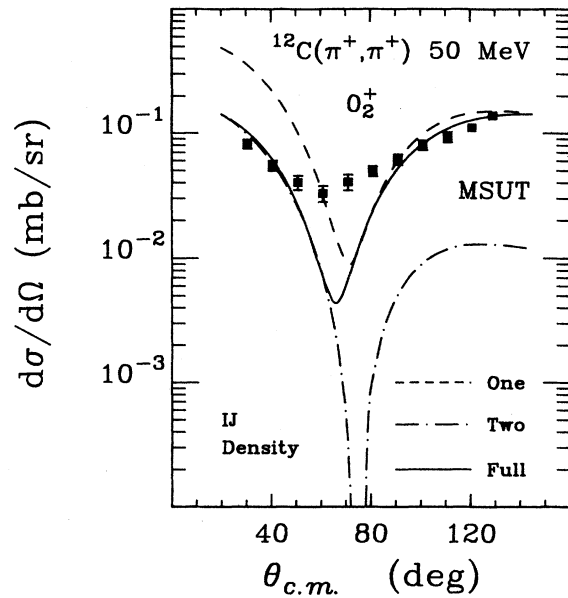


FIG. 7. The direct and two-step  $0_2^+$  cross sections compared with the full 50 MeV calculation.

tions, this difference produces a factor of 2 or 3 in the cross section.

The two-step cross section exhibits a very deep minimum at about  $75^\circ$ , coinciding with the minimum in the  $2^+$  data. For angles larger than this, the two-step contribution to the total cross section is very small. However, for smaller angles the one- and two-step cross

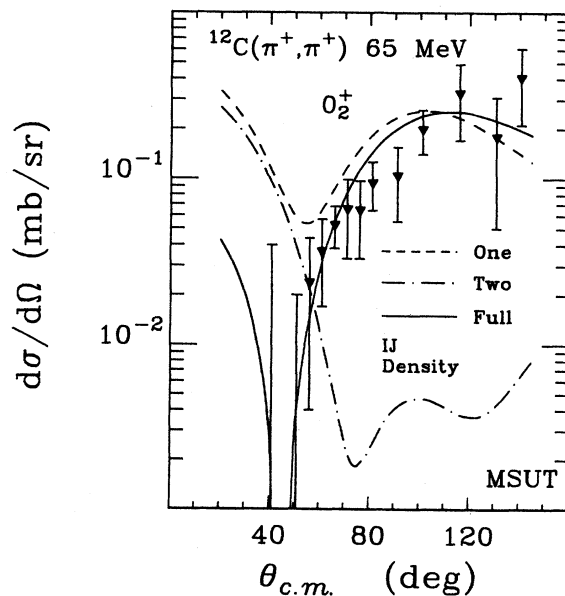


FIG. 8. Same as Fig. 7 but for 65 MeV.

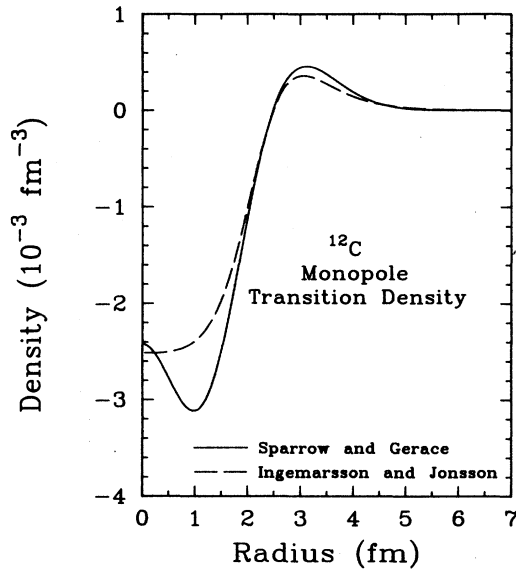


FIG. 9. The monopole transition densities used in the present calculations.

sections are comparable, and their destructive interference gives the required suppression and shifts the minimum to the correct location. The direct transition alone cannot reproduce the forward angle data at either energy and places the minimum at too large an angle.

For comparison the calculations have been repeated using the monopole transition density given by Sparrow and Gerace<sup>1</sup>(SG). This density assumes a modified har-

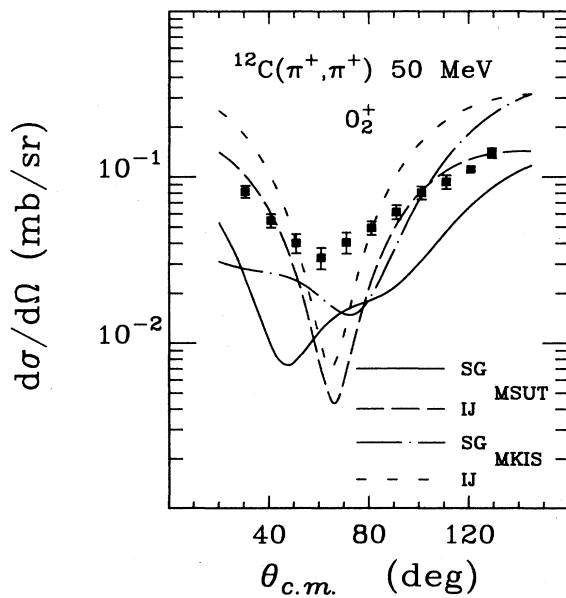


FIG. 10. The 50 MeV monopole cross sections produced by the MSUT and MKIS potentials and the SG and IJ monopole densities. The  $0_2^+$  state is coupled to both the ground and  $2^+$  states.

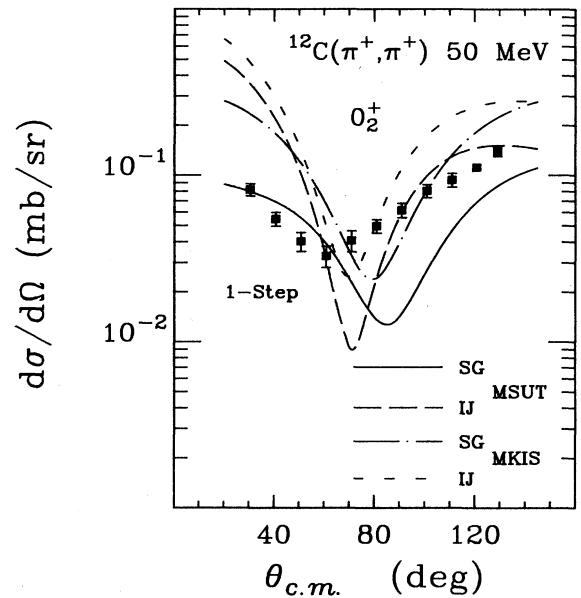


FIG. 11. The same as Fig. 10 except the  $2_1^+ \rightarrow 0_2^+$  coupling is omitted.

monic oscillator shape for the nucleus, and has the form

$$\delta\rho_0(r) = (b\sqrt{\pi})^{-3} [A + B(r/b)^2 + C(r/b)^4] e^{-(r/b)^2}$$

where the oscillator length  $b$  and the constants  $A$ ,  $B$ , and  $C$  are fit to the electromagnetic data. The requirement of orthogonality between the initial and final states reduces the number of independent parameters to three. The parameters determined by Sparrow and Gerace and used

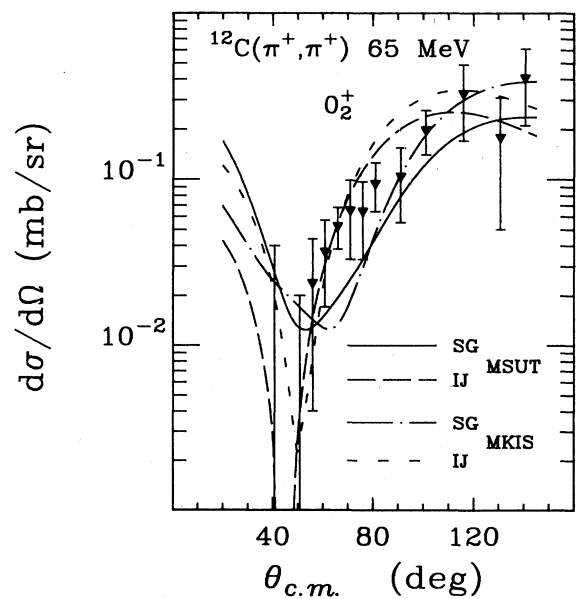


FIG. 12. The same as Fig. 10 but for 65 MeV.

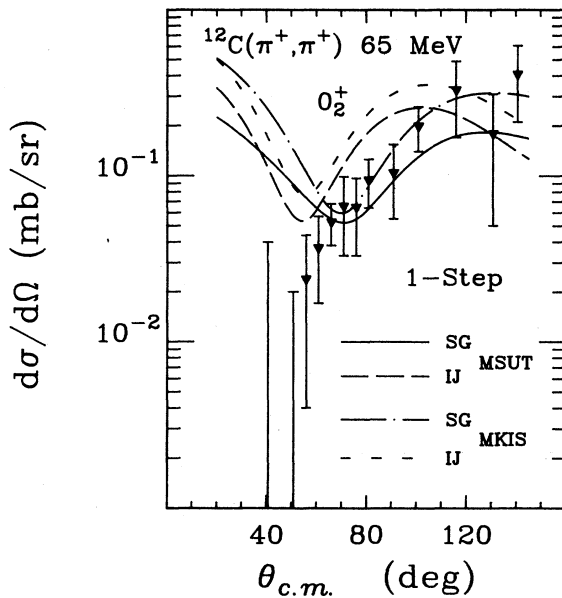


FIG. 13. The same as Fig. 11 but for 65 MeV.

here are  $A = -0.0579$ ,  $B = 0.1652$ ,  $C = 0.0815$ , and  $b = 1.625$  fm.

The two monopole densities are shown in Fig. 9. Both have positive and negative sections as required by orthogonality. They differ most for radii less than about 2 fm. The IJ density, by construction, is constant near  $r = 0$ , while the SG shape has a pronounced minimum at 1 fm.

In Fig. 10 the monopole cross section at 50 MeV, calculated with both potentials and both densities in the full calculation, are compared. The SG density gives a very different angular distribution than the IJ. The MSUT/SG combination gives a minimum near  $45^\circ$ , while the MKIS/SG calculation produces a minimum near  $70^\circ$ . Both calculations underestimate the data at all but the largest angles. The minimum in the SG density near 1 fm increases the overlap between the direct and double-quadrupole transitions, making the cancellation more complete. This lowers the calculated cross section below the data.

Figure 11 shows the cross sections obtained with the direct transition only. The MSUT/SG calculation is much lower than the other three combinations of potential and density. The SG density is similar to the one used by Lee *et al.* in the DW analysis of this data. As in that investigation, including the LLEE correction with this density will give agreement with the data at forward angles. However, the agreement with the location of the minimum and the magnitude of the large angle data is lost.

The full calculation with the four potential/density combinations at 65 MeV is shown in Fig. 12. Here, all the calculations give reasonable agreement with the data. The minima produced by the SG density are more shal-

low than that given by the IJ and shifted to larger angles. The larger error bars do not permit a discrimination among the calculations.

The 65 MeV one-step cross sections are shown in Fig. 13. Clearly, no combination of potential and density gives the required suppression at the forward angles. This is only achieved by the one- and two-step interference.

## CONCLUSIONS

The monopole cross sections calculated with any combination of potential and monopole density discussed here do not describe the data at both 50 and 65 MeV unless both one- and two-step excitation mechanisms are included. The one-step MSUT/SG calculation gives agreement at forward angles at 50 MeV but is too large at 65 MeV. In none of the one-step calculations is the location or the energy dependence of the minimum given correctly. A consistent description of the monopole cross section is only obtained by the full CC calculation.

The variations observed in both the one-step and full calculations introduced by different choices for the monopole transition density make discrimination of the optical models difficult. Comparing the MSUT and MKIS forward angle cross sections at 50 MeV with the data indicate a preference for the MSUT calculation. Certainly a more sophisticated calculation which correctly accounts for the particle-hole character of the  $0_2^+$  states and a more realistic  $2_1^+ \rightarrow 0_2^+$  transition density can be made, but the quality and quantity of the data are, at present, the limiting factor.

The difference between the two optical models for the  $0_1^+$  and  $2_1^+$  states, particularly at 50 MeV, also tends to confirm the need for the more complete potential. However, as already discussed, this difference can be removed by a different choice of phenomenological parameters and deformation length. The static limit on the  $p$ -wave strength required for the MKIS fits can be removed in a finite range model. At present no coupled channels code is available to examine inelastic scattering with such a potential. The present work provides a reference for comparison when finite range codes become available.

Extracting detailed information concerning the optical model from inelastic scattering requires a careful treatment of the nuclear structure and an analysis of data from more than one energy. The monopole transition is sensitive to the optical potential at forward angles because the direct transition here is determined by the distortions. But precisely for this reason, the calculated angular distributions are sensitive to changes in these distortions introduced by the couplings between the states as well as the interference of competing channels.

This work was supported in part by the National Science Foundation.



- \*Present address: Building 510A, Physics Department, Brookhaven National Laboratory, Upton, NY 11973.
- <sup>1</sup>D. A. Sparrow and W. J. Gerace, *Phys. Rev. Lett.* **41**, 1101 (1978).
  - <sup>2</sup>D. A. Sparrow and W. J. Gerace, *Phys. Rev. C* **29**, 949 (1984).
  - <sup>3</sup>L. Lee, T. E. Drake, L. Buchmann, A. Galindo-Uribarri, R. Schubank, R. J. Sobie, D. R. Gill, B. K. Jennings, and N. De Takacsy, *Phys. Lett. B* **174**, 147 (1986).
  - <sup>4</sup>B. K. Jennings and N. de Takacsy, *Phys. Lett.* **124B**, 302 (1983).
  - <sup>5</sup>C. S. Whisnant, G. S. Adams, C. S. Mishra, J. A. Escalante, M. Al-Solami, B. M. Preedom, B. G. Ritchie, and D. H. Wright, *Phys. Rev. C* **39**, 1935 (1989).
  - <sup>6</sup>H. L. Crannell and T. A. Griffy, *Phys. Rev.* **136**, B1580 (1964).
  - <sup>7</sup>Jerome H. Fergeau, *Phys. Rev.* **104**, 225 (1956).
  - <sup>8</sup>H. L. Crannell, *Phys. Rev.* **148**, 1107 (1966).
  - <sup>9</sup>P. Strehl, *Z. Phys.* **234**, 416 (1970).
  - <sup>10</sup>J. F. Amann, P. D. Barnes, K. G. R. Doss, S. A. Dytman, R. A. Eisenstein, J. D. Sherman, and W. R. Wharton, *Phys. Rev. C* **23**, 1635 (1981).
  - <sup>11</sup>K. Stricker, H. McManus, and J. A. Carr, *Phys. Rev. C* **19**, 929 (1979).
  - <sup>12</sup>R. Seki and K. Masutani, *Phys. Rev. C* **27**, 2799 (1983).
  - <sup>13</sup>R. Seki, K. Masutani, and K. Yazaki, *Phys. Rev. C* **27**, 2817 (1983).
  - <sup>14</sup>K. Stricker, J. A. Carr, and H. McManus, *Phys. Rev. C* **22**, 2043 (1980).
  - <sup>15</sup>J. A. Carr, H. McManus, and K. Stricker-Bauer, *Phys. Rev. C* **25**, 952 (1982).
  - <sup>16</sup>C. Steven Whisnant, *Phys. Rev. C* **34**, 262 (1986).
  - <sup>17</sup>R. J. Sobie, T. E. Drake, K. L. Erdman, R. R. Johnson, H. W. Roser, R. Tacik, E. W. Blackmore, D. R. Gill, S. Martin, C. A. Wiedner, and T. Masterson, *Phys. Rev. C* **30**, 1612 (1984).
  - <sup>18</sup>C. Steven Whisnant, *Phys. Rev. C* **33**, 1443 (1986).
  - <sup>19</sup>U. Wienands, N. Hessey, B. M. Barnett, F. M. Rozon, H. W. Roser, A. Altman, R. R. Johnson, D. R. Gill, G. R. Smith, C. A. Wiedner, D. M. Manley, B. L. Berman, H. J. Crawford, and N. Grion, *Phys. Rev. C* **35**, 708 (1987).
  - <sup>20</sup>B. Fick, M. Blecher, K. Gotow, D. Wright, R. L. Boudrie, R. L. Burman, D. Mack, B. G. Ritchie, P. G. Roos, J. A. Escalante, C. S. Mishra, B. M. Preedom, and C. S. Whisnant, *Phys. Rev. C* **34**, 643 (1986).
  - <sup>21</sup>C. S. Mishra, B. Fick, M. Blecher, W. Burger, R. L. Burman, G. Ciangaru, J. Escalante, K. Gotow, M. V. Hynes, B. M. Preedom, B. G. Ritchie, C. S. Whisnant, and D. H. Wright, *Phys. Rev. C* **38**, 1316 (1988).
  - <sup>22</sup>Mikkel B. Johnson and H. A. Bethe, *Nucl. Phys.* **A305**, 418 (1978).
  - <sup>23</sup>T.E.O. Ericson and F. Myhrer, *Phys. Lett.* **74B**, 163 (1978).
  - <sup>24</sup>C. W. De Jager, H. De Vries, and C. De Vries, *At. Data Nucl. Data Tables*, **14**, 479 (1974).
  - <sup>25</sup>B. M. Preedom, S. H. Dam, C. W. Darden III, R. D. Edge, R. L. Burman, H. Hamm, M. A. Moinester, R. P. Redwine, M. A. Yates, F. E. Bertrand, T. P. Clearly, E. E. Gross, N. W. Hill, C. A. Ludeman, M. Blecher, K. Gotow, D. Jenkins, and F. Milder, *Phys. Rev. C* **23**, 1134 (1981).
  - <sup>26</sup>M. Blecher, K. Gotow, R. L. Burman, M. V. Hynes, M. L. Leitch, N. S. Chant, L. Rees, P. G. Roos, F. E. Bertrand, E. E. Gross, F. E. Obenshain, T. P. Sjoreen, G. S. Blanpied, B. M. Preedom, and B. G. Ritchie, *Phys. Rev. C* **28**, 2033 (1983).
  - <sup>27</sup>S. A. Dytman, J. F. Amann, P. D. Barnes, J. N. Craig, K. G. R. Doss, R. A. Eisenstein, J. D. Sherman, W. R. Wharton, G. R. Burleson, S. L. Verbeck, R. J. Peterson, and H. A. Thiessen, *Phys. Rev. C* **19**, 971 (1979).
  - <sup>28</sup>A. Ingemarsson and O. Jonsson, *Nucl. Phys.* **A388**, 644 (1982).
  - <sup>29</sup>G. S. Blanpied, G. W. Hoffmann, M. L. Bartlett, J. A. McGill, S. J. Greene, L. Ray, O. B. Van Dyck, J. Amann, and H. A. Thiessen, *Phys. Rev. C* **23**, 2599 (1981).
  - <sup>30</sup>A. Ingemarsson, O. Jonsson, and A. Hallgren, *Nucl. Phys.* **A319**, 377 (1979).
  - <sup>31</sup>G. R. Satchler, *Direct Nuclear Reactions* (Clarendon, New York, 1983), pp. 586–589.
  - <sup>32</sup>A. Ingemarsson and H. V. von Geramb, *Phys. Scr.* **37**, 530 (1988).